Engineering Science & Technology
http://ojs.wiserpub.com/index.php/EST/

UNIVERSAL WISER PUBLISHER

Research Article

In-Plane Analysis of Micro-Cracks Using Modified Couple-Stress Elasticity

J. P. Vafa[1], A. M. Baghestani[2], S. J. Fariborz[1*]

[1]Department of Mechanical Engineering, Amirkabir University of Technology (Tehran Polytechnic), Tehran, Iran
[2]Department of Mechanical Engineering, Babol Noshirvani University of Technology, Babol, Iran
Email: sjfariborz@yahoo.com

Received: 29 October 2024; **Revised:** 7 December 2024; **Accepted:** 17 December 2024

Abstract: Based upon the modified couple stress theory, we devise a procedure to analyze multiple interacting micro-cracks subject to the mixed mode deformation in an isotropic elastic plane. First, we carry out the asymptotic analysis of the displacement field at the tip of a stationary crack. The dominant term of displacement field reveals that the symmetric part of the stress tensor, which is energy conjugate to the strain tensor, is not singular. In contrast, the couple stress tensor has square root singularity at a crack tip. Furthermore, we use the Fourier integral transform to obtain the solution to an edge dislocation in an isotropic plane. Asymptotic analysis of the obtained solutions shows Cauchy singularity in the location of the edge dislocation. The integral equations for several interacting parallel micro-cracks are constructed via the distributed dislocation technique. These equations are solved numerically for the density of dislocations on a micro-crack surface. The effects of intrinsic material length scale on the stress field of a crack and the interaction between two parallel micro-cracks are studied.

Keywords: micro-crack, couple stress, asymptotic analysis, distributed dislocations, singular integral equations

Nomenclature

a	Half crack length
A, B, C, D	Constants of integration
$b_x^{(i)}, b_y^{(i)}$	Dislocation densities for in-plane deformation
$b_\phi^{(i)}$	Disclination density for in-plane deformation
B_x, B_y	Burgers vector of an edge dislocation
B_ϕ	Burger vector of a wedge disclination
e_r, e_θ, e_z	Unit base vectors in cylindrical coordinate system
$\boldsymbol{E}$	Strain tensor
f, g	Defined functions
$\mathcal{F}[\ ;\beta]$	Complex Fourier transform
$g_x^{(i)}, g_y^{(i)}, g_\phi^{(i)}$	Defined bounded functions for dislocation densities
G	Lame's constant of elastic isotropic material
$\overline{G}_t, G_t$	Kernels of integral equations

DOI: https://doi.org/10.37256/est.6120255993

$H(x)$	Heaviside step function
i	Imaginary unit in complex numbers
$\boldsymbol{I}$	Unit matrix
$K_n(x)$	Modified Bessel function of the second kind
$K_R^{(i)}$, $K_L^{(i)}$	Defined couple stress intensity factors
l	Intrinsic length-scale of an elastic isotropic material
$\boldsymbol{m}$	Deviatoric part of couple stress tensor
m_{nn}	Normal component of the couple stress vector
m_{rr}, $m_{r\theta}$, ...	Deviatoric couple stress tensor components
n	Outward unit vector normal to the boundary
N	Number of cracks
p_k^u	Colocation points for solving integral equation
q_k^u	Quadrature points for solving integral equation
r	Polar coordinate system component
$\text{sgn}(x)$	Sign function
t^n	Traction vector
t_{xy}, t_{yy}, ...	Traction vectors components
u, v, w	Displacement components in cylindrical coordinate system
U	Displacement vector
V	Volume of elastic body
W	Strain energy function of elastic body
x, y	Components of Cartesian coordinate system
x_i^0, y_i^0	Coordinates of the center of ith crack
$x_i(p)$, $y_i(p)$	Cracks parametric form in Cartesian coordinate system
α	Apex angle of a wedge
β	Complex Fourier transform parameter
$\delta(x)$	Dirac delta function
ϵ	Levi-Civita permutation symbol
θ	Polar coordinate system component
Θ	Rotation vector
λ	Lame's constant of elastic isotropic material
$\boldsymbol{\sigma}$	Symmetric part of stress tensor
σ_0	Component of applied traction
σ_{rr}, $\sigma_{r\theta}$, $\sigma_{\theta\theta}$, ...	Stress tensor components
$\boldsymbol{\chi}$	Symmetric curvature tensor
ω	Defined elastic isotropic material constant
$\partial(\,)/\partial(\,)$	Partial derivative with respect to the variable
∇	Vector differential operator
$\lvert\,\rvert$	Absolute value
$(\,)^T$	Transpose of a matrix
$(\,)_{,\,()}$	Partial derivatives with respect to the variable
$(\,)'$, $(\,)''$, $(\,)'''$	1st, 2nd and 3rd derivative of a function

1. Introduction

Stress analysis in the micron scales necessitates the consideration of the intrinsic material parameters to relax the locality assumption of the conventional continuum mechanics. The microstructural effect on the mechanical behavior of solids, such as those with coarse grains, glassy and semi-crystalline polymers [1], porous materials [2], and foams [3] is well-known. In polycrystalline materials, the existence of micro-cracks is inevitable. Experimental results indicated that

bodies containing micro-cracks were more resistant to fracture than those with macro-cracks [4]. However, the classical elasticity theory is insensitive to the length scale, leading to the application of the non-classical elasticity theories [5]. We provide a brief review of studies that used strain gradient elasticity, and couple stress theories to model material length scale effects in crack problems. The earliest attempt to incorporate material length scale into the analysis was made by Sternberg and Muki [6]. They considered the plane strain formulation of couple-stress theory, devised initially by Mindlin [7] for the two-dimensional problems, to analyze cracks under a uniformly distributed uniaxial tension and obtain a singular stress field at the crack tips. Han et al. [8] obtained dynamic stress and dynamic couple stress intensity factors for a finite crack which may propagate under mode I loading. Anisotropic strain gradient formulation was used by Vardoulakis et al. [9] for mode III analysis of a crack. A mixed-mode crack problem was solved by Huang et al. [10] by considering strain gradient effects. They showed that near-tip stress and couple-stress fields were square-root singular. The fracture of cellular materials employing gradient elasticity was addressed by Chen et al. [11]. Paulino et al. [12] and Chan et al. [13] considered mode III deformation of a crack in a functionally graded material using gradient elasticity theory. In the framework of couple stress elasticity theory developed by Koiter [14], the anti-plane deformation of a crack situated at the interface of two dissimilar planes was analyzed by Piccolroaz et al. [15]. Their major finding was that stress singularity at the crack tip was strongly influenced by microstructural parameters and may or may not exhibit oscillatory behavior. The same elasticity theory was employed by Mishuris et al. [16] to address the problem of steady-state propagation of a semi-infinite crack subject to anti-plane loading. The couple stress theory was used by Itou [17] for the analysis of elastic layers containing a crack perpendicular to the boundary. Layers were under uniform tensile traction and the effect of couple stress on crack stress intensity factors was investigated. Karimpour and Fotuhi [18] studied the anti-plane deformation of a cracked plane utilizing strain gradient theory. The above problem was solved by Zhao et al. [19] in the framework of a modified strain gradient model leading to a stress field with singularity stronger than square root. In two articles Baxevanakis et al. [20]-[21], considered the interaction of a discrete dislocation and a finite length crack using couple stress elasticity. Opening and shear modes were studied, respectively, in the first and second articles. Vafa and Faiborz [22] considered micro-cracks under anti-plane deformation based on the modified couple stress theory. They analyzed a screw dislocation in a plane and then employed a dislocation distributed method to study the anti-plane deformation of multiple cracks in the plane. Gourgiotis [23], in the context of couple stress theory, studied the interaction of two collinear in-plane cracks under remotely applied shear traction. The effects of material characteristic length on cracks stress intensity factors and energy release rates were also investigated. Homayounfard et al. [24] presented a finite element formulation for studying mode I crack problems within couple stress elasticity. They studied a crack in an infinite and finite-width plate. Moreover, the effects of internal length parameters on stress, couple stress intensity factors, and energy release rate were examined. Joseph et al. [25] used strain gradient elasticity theory to deal with a crack in a layer under anti-plane deformation. Li and Wang [26] analyzed the same problem in a layer sandwiched between two semi-infinite layers. Gharahi and Schiavone [27] used the micropolar surface model to analyze the deformation of a micropolar half-plane weakened by a single-edge dislocation. Nobili et al. [28] analyzed the elasto-dynamic anti-plane deformation of a semi-infinite crack utilizing couple stress theory by taking into account the micro inertia. Baxevanakis and Georgiadis [29] considered the interaction of a finite-length crack with climb, glide, and screw dislocation dipoles. In all cases, the defects are placed along the crack plane and are not emitted by the crack tip. Giannakopoulos and Zisis [30] studied a moving semi-infinite crack in an infinite flexoelectric material with constant velocity. They showed that the anti-plane dynamic flexoelectric problem is equivalent to a dynamic couple stress elasticity problem. Employing William's expansion method Tian et al. [31] analyzed the electromechanical coupling effect around the tip of a crack under anti-plane deformation. Lei et al. [32] developed general displacement and traction boundary integral equations to analyze plane strain problems of three typical couple stress theories. They considered some numerical examples using the boundary element method, including a center crack in a plate. Cong and Duc [33] studied the mode I crack propagation problem using the modified couple stress and the phase-field theory. Chen et al. [34] investigated a mode I embedded crack in a pre-stressed elastic medium using couple stress theory. They analyzed the effects of material parameters and initial stress by numerically solving the governing equations with the Fourier transform method. Chen et al. [35] analyzed an interface crack between two pre-stressed couple stress materials under an anti-plane shear load. Lazar [36] used nonlocal simplified first strain gradient elasticity theory to solve the screw and edge dislocation problem in a plane and showed that all relevant dislocation fields are nonsingular. Solyaev [37] derived an asymptotic solution for the higher-order mode I crack tip fields using strain gradient elasticity theory. Chen et

al. [38] used couple stress theory to solve a Yoffe-type anti-plane crack problem with a couple of tractions on the crack surface. Xie and Linder [39] obtained the full-field solution for mode III deformation of semi-infinite and finite cracks in flexoelectric solids. The mode III fracture of a Yoffe crack in flexoelectric materials was the subject of study by Knisovitis et al. [40]. They studied the asymptotic structure of the displacement and the polarization fields at the crack tip.

In the present article, the study in Vafa and Fariborz [22], is extended to the in-plane case. The modified couple-stress theory [41] is employed for the in-plane analysis of multiple micro-cracks in an isotropic elastic plane. It is worth mentioning that among several well-known non-local theories, the modified couple stress theory is attractive because it involves only one material length-scale parameter, its boundary conditions are derived using the principle of virtual work, and the stress tensors used in the expression for strain energy density are symmetrical. The asymptotic analysis is carried out to derive the dominant solution of the displacement field in the inner region of the crack tip. The results show that in contrast to the local elasticity theory at the tip of a crack, the symmetric part of the stress tensor is not singular. Furthermore, we solved the edge dislocation problem in an isotropic plane and observed that the resultant stress components are Cauchy singular. Then, via the distributed dislocation technique [42], the integral equations are derived for multiple interacting micro-cracks in the isotropic planes. The numerical solutions to these equations are used to study the effect of intrinsic material length scale on stress distribution and the interaction between two parallel micro-cracks.

2. Formulation of the modified couple stress elasticity

We review the basic three-dimensional formulation of the modified couple-stress elasticity. Then the formulation is simplified for a two-dimensional case to be used in analyzing elastic wedge and edge dislocation problems.

2.1 *Three-dimensional formulation*

In the framework of modified couple stress elasticity, in a linear elastic body with volume V, the strain energy density function W is expressed as [41]

$$W = \frac{1}{2}\int_V (\boldsymbol{E} : \boldsymbol{\sigma} + \boldsymbol{\chi} : \boldsymbol{m})\, dV \tag{1}$$

where $\boldsymbol{\sigma}$ is the symmetric part of the stress tensor, and $\boldsymbol{m}$ is the deviatoric part of the couple stress tensor, and their conjugate deformations are $\boldsymbol{E}$, the strain, and $\boldsymbol{\chi}$, the symmetric curvature tensors, respectively. Therefore, in this theory, the strain energy function does not depend explicitly on anti-symmetric parts of the curvature and stress tensors. The strain and curvature tensors in terms of displacement vector U are represented as

$$\boldsymbol{E} = \frac{1}{2}\left[\nabla U + (\nabla U)^T\right]$$

$$\boldsymbol{\chi} = \frac{1}{2}\left[\nabla \Theta + (\nabla \Theta)^T\right] \tag{2}$$

where ∇ is the vector differential operator, superscript T designates the transpose of a matrix, and Θ is the rotation vector defined as

$$\Theta = \frac{1}{2}\nabla \times U \tag{3}$$

The constitutive equations for elastic isotropic materials in the modified couple-stress elasticity involve only one intrinsic length-scale l and read

$$\boldsymbol{\sigma} = \lambda \,\mathrm{tr}(\boldsymbol{E})\boldsymbol{I} + 2G\boldsymbol{E}$$

$$\boldsymbol{m} = 2Gl^2\boldsymbol{\chi} \tag{4}$$

where λ and G are the Lame's constants and $\boldsymbol{I}$ is the unit matrix. It is worth mentioning that the value of the intrinsic length scale depends upon the micro-structure of materials. Conducting the torsion test on thin copper wires [43] found the mean value of $l = 3.7\ \mu m$ for the material. Li et al. [44] presented a standard experimental method for measuring l and obtained its value for copper and titanium micro-beams.

The equilibrium equations, ignoring body-force and -couple, yield

$$\nabla\cdot\boldsymbol{\sigma} + \frac{1}{2}\epsilon : \nabla\nabla\cdot\boldsymbol{m} = 0 \tag{5}$$

where ϵ is the Levi-Civita permutation symbol. The five boundary conditions required in the couple stress elasticity problems are

$$\text{either } U = \text{known or } t^n = t_{jn}e_j = n\cdot\boldsymbol{\sigma} + \frac{1}{2}n\times\left(\nabla\cdot\boldsymbol{m} - \nabla m_{nn}\right) = \text{known}$$

$$\text{either } \Theta\cdot(\boldsymbol{I} - nn) = \text{known or } m^n = n\cdot m\cdot(\boldsymbol{I} - nn) = \text{known} \tag{6}$$

In Eq (6), n is the outward unit vector normal to the boundary and $m_{nn} = n\cdot m\cdot n$ is the normal component of the couple stress vector.

2.2 *Two-dimensional formulation*

The above formulation, in tensor form, is simplified in the generalized plane-strain elasticity problems [45]. Employing cylindrical coordinates, the displacement vector may be expressed as

$$U = u(r,\theta)e_r + v(r,\theta)e_\theta + w(r,\theta)e_z \tag{7}$$

In Eq (7), e_r, e_θ, and e_z are unit base vectors. The vector differential operator is simplified as

$$\nabla = e_r\frac{\partial}{\partial r} + \frac{e_\theta}{r}\frac{\partial}{\partial\theta} \tag{8}$$

By Eqs (2)-(5) and (7)-(8), equilibrium equations in terms of the displacement components, yield

$$(\lambda+2G)\left[u_{,r} + \frac{u + v_{,\theta}}{r}\right]_{,r} - \frac{G}{r}\left[v_{,r} + \frac{v - u_{,\theta}}{r}\right]_{,\theta}$$

$$+\frac{Gl^2}{4r^4}\left\{r^3v_{,rr\theta} + r^2\left(2v_{,rr\theta} - u_{,rr\theta\theta}\right) + r\left(u_{,r\theta\theta} - v_{,r\theta} + v_{,r\theta\theta\theta}\right) - u_{,\theta\theta\theta\theta} + v_{,\theta\theta\theta} - u_{,\theta\theta} + v_{,\theta}\right\} = 0,$$

$$\frac{\lambda+2G}{r}\left[u_{,r}+\frac{u+v_{,\theta}}{r}\right]_{,\theta}+G\left[v_{,r}+\frac{v-u_{,\theta}}{r}\right]_{,r}$$

$$-\frac{Gl^2}{4r^4}\left\{r^4v_{,rrrr}+r^3\left(2v_{,rrr}-u_{,rrr\theta}\right)+r^2\left(2u_{,rr\theta}-3v_{,rr}+v_{,rr\theta\theta}\right)\right.$$

$$\left.+r\left(3v_{,r}-3u_{,r\theta}-v_{,r\theta\theta}-u_{,r\theta\theta\theta}\right)+3\left(u_{,\theta\theta\theta}-v_{,\theta\theta}+u_{,\theta}-v\right)\right\}=0,$$

$$w_{,rr}+\frac{w_{,r}}{r}+\frac{w_{,\theta\theta}}{r^2}-\frac{l^2}{4r^4}\left\{r^4w_{,rrrr}+2r^3w_{,rrr}+r^2\left(2w_{,rr\theta\theta}-w_{,rr}\right)\right.$$

$$\left.+r\left(w_{,r}-2w_{,r\theta\theta}\right)+w_{,\theta\theta\theta\theta}+4w_{,\theta\theta}\right\}$$

$$=(\nabla\cdot\nabla)w-\frac{l^2}{4}(\nabla\cdot\nabla)^2w=0 \tag{9}$$

In Eq (9), subscripts following a comma signify partial derivatives with respect to the variables. From Eq (6), in an infinite wedge with apex angle α, the conditions on the boundary $\theta = (0, \alpha)$ become

$$\text{either } ue_r+ve_\theta+we_z=\text{known or }\left[\sigma_{r\theta}+\frac{1}{2}\left(m_{rz,r}+\frac{m_{rz}+m_{\theta z,\theta}}{r}\right)\right]e_r+\sigma_{\theta\theta}e_\theta$$

$$+\left[\sigma_{\theta z}-\frac{1}{2}\left(m_{rr,r}-m_{\theta\theta,r}+\frac{m_{rr}-m_{\theta\theta}+m_{\theta r,\theta}}{r}\right)\right]e_z=\text{known}$$

$$\text{either } \Theta_re_r+\Theta_ze_z=\text{ known or } m_{\theta r}e_r+m_{\theta z}e_z=\text{known} \tag{10}$$

These conditions, in terms of displacement components, may be expressed as

$$\text{either } u=\text{known or } \frac{G}{4r^3}\left\{\left(l^2-4r^2\right)\left(v-u_{,\theta}-rv_{,r}\right)\right.$$

$$\left.+l^2\left(r^3v_{,rrr}+2r^2v_{,rr}-r^2u_{,rr\theta}+ru_{,r\theta}+rv_{,r\theta\theta}+v_{,\theta\theta}-u_{,\theta\theta\theta}\right)\right\}=\text{known}$$

$$\text{either } v=\text{known or } \lambda u_{,r}+\frac{\lambda+2G}{r}\left(u+v_{,\theta}\right)=\text{known}$$

$$\text{either } w=\text{known or } \frac{G}{r}\left\{w_{,\theta}-\frac{l^2}{4r^2}\left(3r^2w_{,rr\theta}-3rw_{,r\theta}+4w_{,\theta}+w_{,\theta\theta\theta}\right)\right\}=\text{known}$$

$$\text{either } \frac{w_{,\theta}}{2r}=\text{known or } -\frac{Gl^2}{2r^2}\left(r^2w_{,rr}-rw_{,r}-w_{,\theta\theta}\right)=\text{known}$$

$$\text{either } \frac{1}{2}\left(v_{,r}+\frac{v-u_{,\theta}}{r}\right)=\text{known or } \frac{Gl^2}{2r^2}\left(rv_{,r\theta}+v_{,\theta}-u_{,\theta\theta}\right)=\text{known} \tag{11}$$

From Eqs (9) and (11), we observe that formulations of in-plane and anti-plane deformations are decoupled. Therefore, these problems may be treated separately. In what follows, the in-plane problem is analyzed.

3. Stress near a wedge apex

We study the behavior of the stress field in the inner region of a wedge apex, Figure 1.

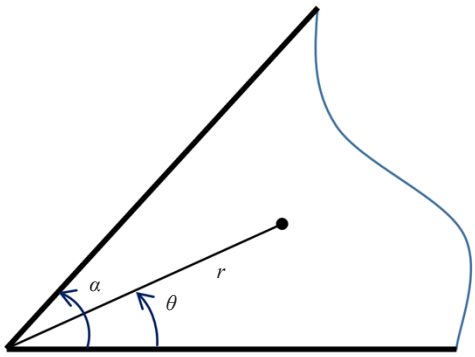

Figure 1. Schematic of the infinite wedge

The strain energy should be finite at the wedge apex which implies, in view of Eqs (1) and (2), that the displacement vector in this region should behave as $U \sim r^{\gamma}F(\theta)$, $\gamma > 1$ as $r \to 0$. By Eqs (2) and (4), this results in the boundedness of the symmetric part of stress tensor $\boldsymbol{\sigma}$ (called, thereafter, stress tensor) in the inner region of wedge apex, i.e., $r/l = \varepsilon \ll 1$. In the following, we investigate the behavior of the stress tensor $\boldsymbol{\sigma}$ and the deviatoric part of the couple stress tensor $\boldsymbol{m}$ (called, thereafter, couple stress tensor) at a wedge apex under in-plane deformation.

In view of Eq (9), in the vicinity of a wedge apex, the dominant equations become

$$r^3v_{,rrr\theta}+r^2\left(2v_{,rr\theta}-u_{,rr\theta\theta}\right)+r\left(u_{,r\theta\theta}-v_{,r\theta}+v_{,r\theta\theta\theta}\right)-u_{,\theta\theta\theta\theta}+v_{,\theta\theta\theta}-u_{,\theta\theta}+v_{,\theta}=0,$$

$$r^4v_{,rrrr}+r^3\left(2v_{,rrr}-u_{,rrr\theta}\right)+r^2\left(2u_{,rr\theta}-3v_{,rr}+v_{,rr\theta\theta}\right)+r\left(3v_{,r}-3u_{,r\theta}-v_{,r\theta\theta}-u_{,r\theta\theta\theta}\right)$$

$$+3\left(u_{,\theta\theta\theta}-v_{,\theta\theta}+u_{,\theta}-v\right)=0 \tag{12}$$

Following Williams [46], the solutions to these equations are taken as

$$u=r^{\gamma}f(\theta),\ v=r^{\gamma}g(\theta) \tag{13}$$

We substitute Eq (13) into (12) and observe that the resultant equations are satisfied provided that

$$f''+(\gamma-1)^2 f=0,\ g''+(\gamma-1)^2 g=0 \tag{14}$$

where $(')=d/d\theta$. The solutions to Eq (14) are readily known

$$f=A\cos(\gamma-1)\theta+B\sin(\gamma-1)\theta$$

$$g=C\cos(\gamma-1)\theta+D\sin(\gamma-1)\theta \tag{15}$$

From Eqs (11) and (13), the boundary conditions for Eq (15) near the tip of a crack, i.e., $0<\theta<2\pi$ are taken as

$$f'''+(\gamma-1)^2 f'=0,\ f''=0$$

$$g''+(\gamma-1)^2 g=0,\ g'=0,\ \text{on } \theta=0,2\pi \tag{16}$$

The application of boundary conditions (16) to Eq (15), considering $\gamma>1$ due to the finiteness of strain energy, leads to

$$\gamma=1+\frac{n}{2},\ n\in\{1,2,3,\ldots\} \tag{17}$$

Therefore, contrary to the local elasticity theory, in the modified couple stress model stress tensor $\boldsymbol{\sigma}$ is bounded at a crack tip whereas couple stress tensor $\boldsymbol{m}$ is square root singular. The asymptotic displacement fields in Eq. (17) align with the crack tip analysis by Aravas and Giannakopoulos [47] for gradient elasticity theory.

4. Edge dislocation solution

Utilizing the modified couple-stress theory, the problem of edge dislocation in an elastic isotropic plane is investigated. In-plane equilibrium Eq (5) in terms of the displacement field in Cartesian coordinates become

$$(\lambda+2G)u_{,xx}+(\lambda+G)v_{,xy}+Gu_{,yy}+\frac{Gl^2}{4}\left[v_{,xxxy}-u_{,xxyy}+v_{,xyyy}-u_{,yyyy}\right]=0$$

$$Gv_{,xx}+(\lambda+G)u_{,xy}+(\lambda+2G)v_{,yy}-\frac{Gl^2}{4}\left[v_{,xxxx}-u_{,xxxy}+v_{,xxyy}-u_{,xyyy}\right]=0 \tag{18}$$

The related geometric and natural boundary conditions on the line $y=$ constant, are obtained by setting $n=e_j$ in Eq (6), resulting in

$$\text{either } u=\text{known or } t_{xy}=\sigma_{xy}+\frac{1}{2}\left(m_{xz,x}+m_{yz,y}\right)=\text{known}$$

$$\text{either } v=\text{known or } t_{yy}=\sigma_{yy}=\text{known}$$

$$\text{either } \Theta_z=\text{known or } m_{yz}=\text{known} \tag{19}$$

The above boundary conditions in terms of displacement components, become

$$\text{either } u = \text{known or } t_{xy} = G\left(u_{,y} + v_{,x}\right) + \frac{Gl^2}{4}\left(v_{,xxx} - u_{,xxy} + v_{,xyy} - u_{yyy}\right) = \text{known}$$

$$\text{either } v = \text{known or } t_{yy} = \lambda u_{,x} + (\lambda + 2G)v_{,y} = \text{known}$$

$$\text{either } \frac{1}{2}\left(v_{,x} - u_{,y}\right) = \text{known or } m_{yz} = \frac{Gl^2}{2}\left(v_{,xy} - u_{,yy}\right) = \text{known} \tag{20}$$

The solution to the edge dislocation with Burgers vector $\boldsymbol{B} = \{\boldsymbol{B}_x, \boldsymbol{B}_y\}$ and wedge disclination $\boldsymbol{B}_\phi$ located at the origin of the coordinate system where the cut is the half-line $\boldsymbol{x} > 0$ in the context of the modified couple-stress theory, is derived. Equation (18) for the in-plane deformation are rewritten as

$$(\omega+2)u_{,xx} + (\omega+1)v_{,xy} + u_{,yy} + \frac{l^2}{4}\left[v_{,xxxy} - u_{,xxyy} + v_{,xyyy} - u_{,yyyy}\right] = 0$$

$$v_{,xx} + (\omega+1)u_{,xy} + (\omega+2)v_{,yy} - \frac{l^2}{4}\left[v_{,xxxx} - u_{,xxxy} + v_{,xxyy} - u_{,xyyy}\right] = 0 \tag{21}$$

where $\omega = \lambda/G$. Utilizing Eq (20), the displacement discontinuity and traction continuity caused by edge dislocation and disclination, on the x-axis are

$$u\left(x,0^+\right) - u\left(x,0^-\right) = B_x H(x),$$

$$v\left(x,0^+\right) - v\left(x,0^-\right) = B_y H(x),$$

$$\frac{1}{2}\left[v_{,x}\left(x,0^+\right) - u_{,y}\left(x,0^+\right)\right] - \frac{1}{2}\left[v_{,x}\left(x,0^-\right) - u_{,y}\left(x,0^-\right)\right] = B_\phi H(x),$$

$$\left[u_{,y}\left(x,0^+\right) + v_{,x}\left(x,0^+\right)\right] + \frac{l^2}{4}\left[v_{,xxx}\left(x,0^+\right) - u_{,xxy}\left(x,0^+\right) + v_{,xyy}\left(x,0^+\right) - u_{,yyy}\left(x,0^+\right)\right]$$

$$= \left[u_{y}\left(x,0^-\right) + v_{,x}\left(x,0^-\right)\right]$$

$$+ \frac{l^2}{4}\left[v_{,xxx}\left(x,0^-\right) - u_{,xxy}\left(x,0^-\right) + v_{,xyy}\left(x,0^-\right) - u_{,yyy}\left(x,0^-\right)\right],$$

$$\omega u_{,x}\left(x,0^+\right) + (\omega+2)v_{,y}\left(x,0^+\right) = \omega u_{,x}\left(x,0^-\right) + (\omega+2)v_{,y}\left(x,0^-\right),$$

$$v_{,xy}\left(x,0^+\right) - u_{,yy}\left(x,0^+\right) = v_{,xy}\left(x,0^-\right) - u_{,yy}\left(x,0^-\right) \tag{22}$$

Applying the complex Fourier transform to Eq (21) and boundary conditions (22), yields

$$\frac{d^2U}{dy^2}+i\beta(\omega+1)\frac{dV}{dy}-\beta^2(\omega+2)U-\frac{l^2}{4}\left[\frac{d^4U}{dy^4}-i\beta\frac{d^3V}{dy^3}-\beta^2\frac{d^2U}{dy^2}+i\beta^3\frac{dV}{dy}\right]=0,$$

$$(\omega+2)\frac{d^2V}{dy^2}+i\beta(\omega+1)\frac{dU}{dy}-\beta^2V+i\beta\frac{l^2}{4}\left[\frac{d^3U}{dy^3}-i\beta\frac{d^2V}{dy^2}-\beta^2\frac{dU}{dy}+i\beta^3V\right]=0,$$

$$U\left(\beta,0^+\right)-U\left(\beta,0^-\right)=B_x\left[\pi\delta(\beta)-\frac{i}{\beta}\right],\ V\left(\beta,0^+\right)-V\left(\beta,0^-\right)=B_y\left[\pi\delta(\beta)-\frac{i}{\beta}\right],$$

$$U_{,y}\left(\beta,0^+\right)-U_{,y}\left(\beta,0^-\right)=\left(i\beta B_y-2B_\phi\right)\left[\pi\delta(\beta)-\frac{i}{\beta}\right],$$

$$V_{,y}\left(\beta,0^+\right)-V_{,y}\left(\beta,0^-\right)=-\frac{i\beta\omega}{\omega+2}B_x\left[\pi\delta(\beta)-\frac{i}{\beta}\right], \tag{23}$$

$$U_{,yy}\left(\beta,0^+\right)-U_{,yy}\left(\beta,0^-\right)=\frac{\omega\beta^2}{\omega+2}B_x\left[\pi\delta(\beta)-\frac{i}{\beta}\right],$$

$$\left[U_{,yyy}\left(\beta,0^+\right)-U_{,yyy}\left(\beta,0^-\right)\right]-i\beta\left[V_{,yy}\left(\beta,0^+\right)-V_{,yy}\left(\beta,0^-\right)\right]$$

$$=2\left[i\beta\frac{4}{l^2}B_y-\left(\beta^2+\frac{4}{l^2}\right)B_\phi\right]\left[\pi\delta(\beta)-\frac{i}{\beta}\right]$$

where $[U(\beta, y), V(\beta, y)] = \mathcal{F}[u(x, y), v(x, y); \beta]$. Taking the inverse Fourier transform of the solution to Eq (23) results in

$$u(x,y)=\frac{B_x}{4}\mathrm{sgn}(y)\left\{1-\frac{1}{\pi}\int_0^\infty\left[\beta l^2e^{-|y|\sqrt{\frac{4}{l^2}+\beta^2}}\left(2\frac{\omega+1}{\omega+2}|y|-\beta l^2-\frac{2}{\beta}\right)e^{-\beta|y|}\right]\sin(\beta x)d\beta\right\}$$

$$-\frac{B_y}{4\pi}\int_0^\infty\left[l^2\sqrt{\frac{4}{l^2}+\beta^2}e^{-|y|\sqrt{\frac{4}{l^2}+\beta^2}}+\left(2\frac{\omega+1}{\omega+2}|y|-\beta l^2-\frac{1}{\beta}\frac{2}{\omega+2}\right)e^{-\beta|y|}\right]\cos(\beta x)d\beta$$

$$+\frac{B_\phi}{4}\left\{le^{-\frac{2}{l}|y|}+\frac{l^2}{\pi}\int_0^\infty\left[\frac{1}{\beta}\sqrt{\frac{4}{l^2}+\beta^2}e^{-|y|\sqrt{\frac{4}{l^2}+\beta^2}}-e^{-\beta|y|}\right]\sin(\beta x)d\beta\right\},$$

$$v(x,y)=-\frac{B_x}{4\pi}\int_0^\infty\left[\frac{\beta^2l^2}{\sqrt{\frac{4}{l^2}+\beta^2}}e^{-|y|\sqrt{\frac{4}{l^2}+\beta^2}}+\left(2\frac{\omega+1}{\omega+2}|y|-\beta l^2+\frac{1}{\beta}\frac{2}{\omega+2}\right)e^{-\beta|y|}\right]\cos(\beta x)d\beta$$

$$+\frac{B_y}{4}\operatorname{sgn}(y)\left\{1+\frac{1}{\pi}\int_0^{\infty}\left[\beta l^2 e^{-|y|\sqrt{\frac{4}{l^2}+\beta^2}}+\left(2\frac{\omega+1}{\omega+2}|y|-\beta l^2+\frac{2}{\beta}\right)e^{-\beta|y|}\right]\sin(\beta x)d\beta\right\}$$

$$-\frac{B_\phi}{4}\operatorname{sgn}(y)\frac{l^2}{\pi}\int_0^{\infty}\left[e^{-\beta|y|}-e^{-|y|\sqrt{\frac{4}{l^2}+\beta^2}}\right]\cos(\beta x)d\beta \tag{24}$$

In light of the identities given in Appendix A, the displacement field (24) is simplified as

$$u(x,y)=\frac{B_x}{2\pi}\left\{\frac{\pi}{2}\operatorname{sgn}(y)-\frac{2xy}{r^2}K_2\left(\frac{2}{l}r\right)-\left(\frac{\omega+1}{\omega+2}\right)\frac{xy}{r^2}+l^2\frac{xy}{r^4}+\tan^{-1}\left(\frac{x}{y}\right)\right\}$$

$$+\frac{B_y}{2\pi}\left\{-\frac{2y^2}{r^2}K_0\left(\frac{2}{l}r\right)+l\frac{x^2-y^2}{r^3}K_1\left(\frac{2}{l}r\right)-\left(\frac{\omega+1}{\omega+2}\right)\frac{y^2}{r^2}-\frac{l^2}{2}\frac{x^2-y^2}{r^4}\right.$$

$$\left.+\frac{1}{\omega+2}\int_0^{\infty}\frac{1}{\beta}e^{-\beta|y|}\cos(\beta x)d\beta\right\}$$

$$+B_\phi\left\{\frac{l}{4}e^{-\frac{2}{l}|y|}+\frac{l^2}{4\pi}\int_0^{\infty}\left[\frac{1}{\beta}\sqrt{\frac{4}{l^2}+\beta^2}\,e^{-|y|\sqrt{\frac{4}{l^2}+\beta^2}}-e^{-\beta|y|}\right]\sin(\beta x)d\beta\right\},$$

$$v(x,y)=\frac{B_x}{2\pi}\left\{\frac{2x^2}{r^2}K_0\left(\frac{2}{l}r\right)+l\frac{x^2-y^2}{r^3}K_1\left(\frac{2}{l}r\right)-\left(\frac{\omega+1}{\omega+2}\right)\frac{y^2}{r^2}-\frac{l^2}{2}\frac{x^2-y^2}{r^4}-\frac{1}{\omega+2}\int_0^{\infty}\frac{1}{\beta}e^{-\beta|y|}\cos(\beta x)d\beta\right\}$$

$$+\frac{B_y}{2\pi}\left\{\frac{\pi}{2}\operatorname{sgn}(y)+\frac{2xy}{r^2}K_2\left(\frac{2}{l}r\right)+\left(\frac{\omega+1}{\omega+2}\right)\frac{xy}{r^2}-l^2\frac{xy}{r^4}+\tan^{-1}\left(\frac{x}{y}\right)\right\}$$

$$+B_\phi\left\{\operatorname{sgn}(y)\frac{l^2}{4\pi}\int_0^{\infty}\left[e^{-|y|\sqrt{\frac{4}{l^2}+\beta^2}}-e^{-\beta|y|}\right]\cos(\beta x)d\beta\right\} \tag{25}$$

The stress and traction components become

$$\sigma_{xx}(x,y)=B_x\frac{G}{\pi}y\left\{\frac{3x^2-y^2}{r^4}\left[2K_0\left(\frac{2r}{l}\right)-\frac{l^2}{r^2}\right]+\frac{2}{l}\left[\frac{2x^2}{r^3}+\frac{l^2\left(3x^2-y^2\right)}{r^5}\right]K_1\left(\frac{2r}{l}\right)+\left(\frac{\omega+1}{\omega+2}\right)\frac{3x^2+y^2}{r^4}\right\}$$

$$-B_y\frac{G}{\pi}x\left\{\frac{x^2-3y^2}{r^4}\left[2K_0\left(\frac{2r}{l}\right)-\frac{l^2}{r^2}\right]-\frac{2}{l}\left[\frac{2y^2}{r^3}-\frac{l^2\left(x^2-3y^2\right)}{r^5}\right]K_1\left(\frac{2r}{l}\right)\right.$$

$$+\left(\frac{\omega+1}{\omega+2}\right)\frac{x^2-y^2}{r^4}\Bigg\}+B_\phi\frac{G}{\pi}\left\{\frac{2y^2}{r^2}K_0\left(\frac{2r}{l}\right)+\frac{l^2}{2}\frac{x^2-y^2}{r^4}\left[1-\frac{2r}{l}K_1\left(\frac{2r}{l}\right)\right]\right\},$$

$$\sigma_{xy}(x,y)=-B_x\frac{G}{\pi}\left\{\frac{x^2-3y^2}{r^4}\left[2K_0\left(\frac{2r}{l}\right)-\frac{l^2}{r^2}\right]+\frac{2}{l}\left[\frac{x^2-y^2}{r^3}+\frac{l^2\left(x^2-3y^2\right)}{r^5}\right]K_1\left(\frac{2r}{l}\right)+\left(\frac{\omega+1}{\omega+2}\right)\frac{x^2-y^2}{r^4}\right\}$$

$$-B_y\frac{G}{\pi}y\left\{\frac{3x^2-y^2}{r^4}\left[2K_0\left(\frac{2r}{l}\right)-\frac{l^2}{r^2}\right]\right.$$

$$\left.+\frac{2}{l}\left[\frac{x^2-y^2}{r^3}+\frac{l^2\left(3x^2-y^2\right)}{r^5}\right]K_1\left(\frac{2r}{l}\right)+\left(\frac{\omega+1}{\omega+2}\right)\frac{x^2-y^2}{r^4}\right\}$$

$$-B_\phi G\,\mathrm{sgn}(y)\left[\frac{1}{2}e^{-\frac{2}{l}|y|}-\frac{1}{2\pi}\int_0^\infty\left(\beta l^2e^{-\beta|y|}-\frac{\beta^2l^2+2}{\beta}e^{-|y|\sqrt{\frac{4}{l^2}+\beta^2}}\right)\sin(\beta x)d\beta\right],$$

$$t_{xy}(x,y)=-B_x\frac{G}{\pi}x\left\{-\frac{l^2\left(x^2-3y^2\right)}{r^6}+\frac{4x^2}{lr^3}K_1\left(\frac{2r}{l}\right)+\frac{2\left(x^2-3y^2\right)}{r^4}K_2\left(\frac{2r}{l}\right)+\left(\frac{\omega+1}{\omega+2}\right)\frac{x^2-y^2}{r^4}\right\}$$

$$-B_y\frac{G}{\pi}y\left\{-\frac{l^2\left(3x^2-y^2\right)}{r^6}+\frac{4x^2}{lr^3}K_1\left(\frac{2r}{l}\right)+\frac{2\left(3x^2-y^2\right)}{r^4}K_2\left(\frac{2r}{l}\right)+\left(\frac{\omega+1}{\omega+2}\right)\frac{x^2-y^2}{r^4}\right\}$$

$$+B_\phi\frac{G}{\pi}\frac{xy}{r^2}\left[\frac{l^2}{r^2}-2K_2\left(\frac{2r}{l}\right)\right],$$

$$\sigma_{yy}(x,y)=-B_x\frac{G}{\pi}y\left\{-\frac{l^2\left(3x^2-y^2\right)}{r^6}+\frac{4x^2}{lr^3}K_1\left(\frac{2r}{l}\right)+\frac{2\left(3x^2-y^2\right)}{r^4}K_2\left(\frac{2r}{l}\right)+\left(\frac{\omega+1}{\omega+2}\right)\frac{x^2-y^2}{r^4}\right\}$$

$$+B_y\frac{G}{\pi}x\left\{-\frac{l^2\left(x^2-3y^2\right)}{r^6}-\frac{4y^2}{lr^3}K_1\left(\frac{2r}{l}\right)+\frac{2\left(x^2-3y^2\right)}{r^4}K_2\left(\frac{2r}{l}\right)-\left(\frac{\omega+1}{\omega+2}\right)\frac{x^2+3y^2}{r^4}\right\}$$

$$-B_\phi\frac{G}{\pi}\left\{\frac{l^2\left(x^2-y^2\right)}{2r^4}-\frac{l}{r}K_1\left(\frac{2r}{l}\right)+\frac{2y^2}{r^2}K_2\left(\frac{2r}{l}\right)\right\},$$

$$m_{yz}(x,y)=B_x\frac{G}{\pi}\frac{xy}{r^2}\left[K_2\left(\frac{2r}{l}\right)-\frac{l^2}{2r^2}\right]+B_y\frac{G}{\pi}\left\{\frac{l^2\left(x^2-y^2\right)}{4r^4}+\frac{y^2}{r^2}K_2\left(\frac{2r}{l}\right)-\frac{l}{2r}K_1\left(\frac{2r}{l}\right)\right\}$$

$$-B_\phi \frac{Gl}{2\pi}\left[\frac{lx}{r^2}+\pi e^{-\frac{2}{l}|y|}+l\int_0^\infty\left(\frac{1}{\beta}\sqrt{\frac{4}{l^2}+\beta^2}\,e^{-|y|\sqrt{\frac{4}{l^2}+\beta^2}}-e^{-\beta|y|}\right)\sin(\beta x)d\beta\right] \tag{26}$$

Utilizing the polar coordinates (r, θ) and the asymptotic formulas for modified Bessel functions with small arguments [48], we observe that at dislocation location, as $r \to 0$

$$t_{xy}(x,y) \sim -B_x\left(\frac{1}{r}\right)-B_y\left(\frac{1}{r}\right)+B_\phi$$

$$\sigma_{yy}(x,y) \sim -B_x\left(\frac{1}{r}\right)-B_y\left(\frac{1}{r}\right)-B_\phi$$

$$m_{yz}(x,y) \sim B_x+B_y-B_\phi\left(\frac{1}{r}\right),\ r\to 0 \tag{27}$$

The above expressions are Cauchy singular at dislocation location which differs from the stress behavior under anti-plane deformation [22].

5. Micro-cracks formulation

We employ the derived dislocation solution to analyze a plane weakened by N interacting micro-cracks with half-length a_i, $i \in \{1, 2, ..., N\}$. The plane is subjected to uniformly distributed traction as $|y| \to \infty$. For the sake of brevity, only horizontal cracks are considered. The cracks are represented in parametric form, as

$$x_i(p) = x_i^0 + a_i p,\ -1 \le p \le 1$$

$$y_i(p) = y_i^0,\ i \in \{1, 2, \ldots, N\} \tag{28}$$

where x_i^0 and y_i^0 are the coordinates of the center of i_{th} crack. The analyses of micro-cracks under in-plane loading are accomplished using the distributed dislocations technique.

The dislocation and disclination densities for in-plane deformation are defined as

$$b_x^{(i)} = \frac{\partial B_x^{(i)}}{\partial x_i},\ b_y^{(i)} = \frac{\partial B_y^{(i)}}{\partial x_i},\ b_\phi^{(i)} = \frac{\partial B_\phi^{(i)}}{\partial x_i},\ i \in \{1, 2, \ldots, N\} \tag{29}$$

The distributed dislocation technique is employed to construct integral equations for a plane containing N horizontal micro-cracks. The resultant integral equations are

$$t_{xy}^{(i)}\left(x_i(p), y_i(p)\right) = \int_{-1}^{1} a_i b_x^{(i)}(q)\overline{G}_{t_{xy}}^{x}\left(x_i(p)-x_i(q)\right)dq$$

$$+\sum_{\substack{j=1\\ j\neq i}}^{N}\int_{-1}^{1} a_j b_x^{(j)}(q)G_{t_{xy}}^{x}\left(x_i(p)-x_j(q), y_i(p)-y_j(q)\right)dq$$

$$+\sum_{\substack{j=1\\ j\neq i}}^{N}\int_{-1}^{1} a_j b_y^{(j)}(q) G_{t_{xy}}^{y}\left(x_i(p)-x_j(q), y_i(p)-y_j(q)\right)dq$$

$$+\sum_{\substack{j=1\\ j\neq i}}^{N}\int_{-1}^{1} a_j b_\phi^{(j)}(q) G_{t_{xy}}^{\phi}\left(x_i(p)-x_j(q), y_i(p)-y_j(q)\right)dq,$$

$$\sigma_{yy}^{(i)}\left(x_i(p), y_i(p)\right) = \int_{-1}^{1} a_i b_y^{(i)}(q)\overline{G}_{\sigma_{yy}}^{y}\left(x_i(p)-x_i(q)\right)dq$$

$$+\int_{-1}^{1} a_i b_\phi^{(i)}(q)\overline{G}_{\sigma_{yy}}^{\phi}\left(x_i(p)-x_i(q)\right)dq$$

$$+\sum_{\substack{j=1\\ j\neq i}}^{N}\int_{-1}^{1} a_j b_x^{(j)}(q) G_{\sigma_{yy}}^{x}\left(x_i(p)-x_j(q), y_i(p)-y_j(q)\right)dq$$

$$+\sum_{\substack{j=1\\ j\neq i}}^{N}\int_{-1}^{1} a_j b_y^{(j)}(q) G_{\sigma_{yy}}^{y}\left(x_i(p)-x_j(q), y_i(p)-y_j(q)\right)dq$$

$$+\sum_{\substack{j=1\\ j\neq i}}^{N}\int_{-1}^{1} a_j b_\phi^{(j)}(q) G_{\sigma_{yy}}^{\phi}\left(x_i(p)-x_j(q), y_i(p)-y_j(q)\right)dq, \tag{30}$$

$$m_{yz}^{(i)}\left(x_i(p), y_i(p)\right) = \int_{-1}^{1} a_i b_y^{(i)}(q)\overline{G}_{m_{yz}}^{y}\left(x_i(p)-x_i(q)\right)dq$$

$$+\int_{-1}^{1} a_i b_\phi^{(i)}(q)\overline{G}_{m_{yz}}^{\phi}\left(x_i(p)-x_i(q)\right)dq$$

$$+\sum_{\substack{j=1\\ j\neq i}}^{N}\int_{-1}^{1} a_j b_x^{(j)}(q) G_{m_{yz}}^{x}\left(x_i(p)-x_j(q), y_i(p)-y_j(q)\right)dq$$

$$+\sum_{\substack{j=1\\ j\neq i}}^{N}\int_{-1}^{1} a_j b_y^{(j)}(q) G_{m_{yz}}^{y}\left(x_i(p)-x_j(q), y_i(p)-y_j(q)\right)dq$$

$$+\sum_{\substack{j=1\\ j\neq i}}^{N}\int_{-1}^{1} a_j b_\phi^{(j)}(q) G_{m_{yz}}^{\phi}\left(x_i(p)-x_j(q), y_i(p)-y_j(q)\right)dq,$$

$$-1 \le p \le 1,\ i \in \{1, 2, \ldots, N\}$$

The kernels of integral equation (30) may be readily deduced from Eq (26). These are specified in Appendix B. It is worth mentioning that only kernels with over-bar are Cauchy singular whereas all other kernels are bounded. Making use of the behavior of dislocation and disclination densities at a crack tip, we take

$$b_x^{(i)}(q)=\sqrt{1-q^2}\,g_x^{(i)},\ b_y^{(i)}(q)=\sqrt{1-q^2}\,g_y^{(i)},\ b_\phi^{(i)}(q)=\frac{1}{\sqrt{1-q^2}}\,g_\phi^{(i)} \tag{31}$$

where unknown functions $g_x^{(i)}$, $g_y^{(i)}$, and $g_\phi^{(i)}$ are bounded. Since only $b_\phi^{(i)}(q)$ is square root singular at a crack tip, Eq (30) should satisfy the following closure condition

$$\int_{-1}^{1} b_\phi^{(i)}(q)dq=0,\ i\in\{1,2,\ldots,N\} \tag{32}$$

The numerical solution of integral equations (30) and (32) is accomplished through the procedure devised by, Erdogan et al. [49]. Substituting equation (31) into (30) and (32) for discretization, the following colocation and quadrature points, designated by superscripts b for $b_x^{(i)}$ and $b_y^{(i)}$ and u for $b_\phi^{(i)}$, are used

$$p_k^b=\cos\left(\frac{2k-1}{n+1}\pi\right),\ k\in\{1,2,\ldots,n+1\}$$

$$q_k^b=\cos\left(\frac{k}{n+1}\pi\right),\ k\in\{1,2,\ldots,n\} \tag{33}$$

and

$$p_k^u=\cos\left(\frac{k}{n}\pi\right),\ k\in\{1,2,\ldots,n-1\}$$

$$q_k^u=\cos\left(\frac{2k-1}{2n}\pi\right),\ k\in\{1,2,\ldots,n\} \tag{34}$$

As we may note, points p_k^b and q_k^b are different from those used under anti-plane mode [22], whereas points p_k^u and q_k^u are the same. The resultant algebraic equations become

$$\sum_{r=1}^{n} a_i\frac{\pi\left[1-\left(q_r^b\right)^2\right]}{n+1}g_x^{(i)}\left(q_r^b\right)\overline{G}_{t_{xy}}^{x}\left(x_i\left(p_k^b\right)-x_i\left(q_r^b\right)\right)$$

$$+\sum_{\substack{j=1\\ j\neq i}}^{N} a_j\sum_{r=1}^{n}\frac{\pi\left[1-\left(q_r^b\right)^2\right]}{n+1}g_x^{(j)}\left(q_r^b\right)G_{t_{xy}}^{x}\left(x_i\left(p_k^b\right)-x_j\left(q_r^b\right),y_i\left(p_k^b\right)-y_j\left(q_r^b\right)\right)$$

$$+\sum_{\substack{j=1\\ j\neq i}}^{N} a_j\sum_{r=1}^{n}\frac{\pi\left[1-\left(q_r^b\right)^2\right]}{n+1}g_y^{(j)}\left(q_r^b\right)G_{t_{xy}}^{y}\left(x_i\left(p_k^b\right)-x_j\left(q_r^b\right),y_i\left(p_k^b\right)-y_j\left(q_r^b\right)\right)$$

$$+\sum_{\substack{j=1\\ j\neq i}}^{N} a_j\sum_{r=1}^{n}\frac{\pi}{n}g_\phi^{(j)}\left(q_r^u\right)G_{t_{xy}}^{\phi}\left(x_i\left(p_k^b\right)-x_j\left(q_r^u\right),y_i\left(p_k^b\right)-y_j\left(q_r^u\right)\right)=t_{xy}^{(i)}\left(x_i\left(p_k^b\right)\right),$$

$$\sum_{r=1}^{n} a_i \frac{\pi\left[1-\left(q_r^b\right)^2\right]}{n+1} g_y^{(i)}\left(q_r^b\right) \bar{G}_{\sigma_{yy}}^{y}\left(x_i\left(p_k^b\right)-x_i\left(q_r^b\right)\right)+\sum_{r=1}^{n} a_i \frac{\pi}{n} g_\phi^{(i)}\left(q_r^u\right) \bar{G}_{\sigma_{yy}}^{\phi}\left(x_i\left(p_k^b\right)-x_i\left(q_r^u\right)\right)$$

$$+\sum_{\substack{j=1 \\ j\neq i}}^{N} a_j \sum_{r=1}^{n} \frac{\pi\left[1-\left(q_r^b\right)^2\right]}{n+1} g_x^{(j)}\left(q_r^b\right) G_{\sigma_{yy}}^{x}\left(x_i\left(p_k^b\right)-x_j\left(q_r^b\right), y_i\left(p_k^b\right)-y_j\left(q_r^b\right)\right)$$

$$+\sum_{\substack{j=1 \\ j\neq i}}^{N} a_j \sum_{r=1}^{n} \frac{\pi\left[1-\left(q_r^b\right)^2\right]}{n+1} g_y^{(j)}\left(q_r^b\right) G_{\sigma_{yy}}^{y}\left(x_i\left(p_k^b\right)-x_j\left(q_r^b\right), y_i\left(p_k^b\right)-y_j\left(q_r^b\right)\right)$$

$$+\sum_{\substack{j=1 \\ j\neq i}}^{N} a_j \sum_{r=1}^{n} \frac{\pi}{n} g_\phi^{(j)}\left(q_r^u\right) G_{\sigma_{yy}}^{\phi}\left(x_i\left(p_k^b\right)-x_j\left(q_r^u\right), y_i\left(p_k^b\right)-y_j\left(q_r^u\right)\right)=\sigma_{yy}^{(i)}\left(p_k^b\right),$$

$$\sum_{r=1}^{n} a_i \frac{\pi\left[1-\left(q_r^b\right)^2\right]}{n+1} g_y^{(i)}\left(q_r^b\right) \bar{G}_{m_{yz}}^{y}\left(x_i\left(p_l^u\right)-x_i\left(q_r^b\right)\right)+\sum_{r=1}^{n} a_i \frac{\pi}{n} g_\phi^{(i)}\left(q_r^u\right) \bar{G}_{m_{yz}}^{\phi}\left(x_i\left(p_l^u\right)-x_i\left(q_r^u\right)\right)$$

$$+\sum_{\substack{j=1 \\ j\neq i}}^{N} a_j \sum_{r=1}^{n} \frac{\pi\left[1-\left(q_r^b\right)^2\right]}{n+1} g_x^{(j)}\left(q_r^b\right) G_{m_{yz}}^{x}\left(x_i\left(p_l^u\right)-x_j\left(q_r^b\right), y_i\left(p_l^u\right)-y_j\left(q_r^b\right)\right)$$

$$+\sum_{\substack{j=1 \\ j\neq i}}^{N} a_j \sum_{r=1}^{n} \frac{\pi\left[1-\left(q_r^b\right)^2\right]}{n+1} g_y^{(j)}\left(q_r^b\right) G_{m_{yz}}^{y}\left(x_i\left(p_l^u\right)-x_j\left(q_r^b\right), y_i\left(p_l^u\right)-y_j\left(q_r^b\right)\right)$$

$$+\sum_{\substack{j=1 \\ j\neq i}}^{N} a_j \sum_{r=1}^{n} \frac{\pi}{n} g_\phi^{(j)}\left(q_r^u\right) G_{m_{yz}}^{\phi}\left(x_i\left(p_l^u\right)-x_j\left(q_r^u\right), y_i\left(p_l^u\right)-y_j\left(q_r^u\right)\right)=m_{yz}^{(i)}\left(p_l^u\right),$$

$$\sum_{r=1}^{n} g_\phi^{(i)}\left(q_r^u\right)=0,\ i\in\{1,2,\ldots,N\},\ k\in\{1,2,\ldots,n\},\ l\in\{1,2,\ldots,n-1\} \tag{35}$$

We solve the above system of $3n$ linear algebraic equations to determine the unknown representing dislocation and disclination densities, at the collocation points. The stress fields in a plane weakened by N interacting parallel micro-cracks are

$$\sigma_{xx}(x,y)=\sum_{j=1}^{N}\sum_{r=1}^{n} a_j \frac{\pi\left[1-\left(q_r^b\right)^2\right]}{n+1} g_x^{(j)}\left(q_r^b\right) G_{\sigma_{xx}}^{x}\left(x-x_j\left(q_r^b\right), y-y_j\left(q_r^b\right)\right)$$

$$+\sum_{j=1}^{N}\sum_{r=1}^{n} a_j \frac{\pi\left[1-\left(q_r^b\right)^2\right]}{n+1} g_y^{(j)}\left(q_r^b\right) G_{\sigma_{xx}}^{y}\left(x-x_j\left(q_r^b\right), y-y_j\left(q_r^b\right)\right)$$

$$+\sum_{j=1}^{N}\sum_{r=1}^{n} a_j \frac{\pi}{n} g_{\phi}^{(j)}\left(q_r^u\right) G_{\sigma_{xx}}^{\phi}\left(x-x_j\left(q_r^u\right), y-y_j\left(q_r^u\right)\right)+\sigma_{xx}^{0}(x,y),$$

$$\sigma_{yy}(x,y)=\sum_{j=1}^{N}\sum_{r=1}^{n} a_j \frac{\pi\left[1-\left(q_r^b\right)^2\right]}{n+1} g_x^{(j)}\left(q_r^b\right) G_{\sigma_{yy}}^{x}\left(x-x_j\left(q_r^b\right), y-y_j\left(q_r^b\right)\right)$$

$$+\sum_{j=1}^{N}\sum_{r=1}^{n} a_j \frac{\pi\left[1-\left(q_r^b\right)^2\right]}{n+1} g_y^{(j)}\left(q_r^b\right) G_{\sigma_{yy}}^{y}\left(x-x_j\left(q_r^b\right), y-y_j\left(q_r^b\right)\right)$$

$$+\sum_{j=1}^{N}\sum_{r=1}^{n} a_j \frac{\pi}{n} g_{\phi}^{(j)}\left(q_r^u\right) G_{\sigma_{yy}}^{\phi}\left(x-x_j\left(q_r^u\right), y-y_j\left(q_r^u\right)\right)+\sigma_{yy}^{0}(x,y),$$

$$\sigma_{xy}(x,y)=\sum_{j=1}^{N}\sum_{r=1}^{n} a_j \frac{\pi\left[1-\left(q_r^b\right)^2\right]}{n+1} g_x^{(j)}\left(q_r^b\right) G_{\sigma_{xy}}^{x}\left(x-x_j\left(q_r^b\right), y-y_j\left(q_r^b\right)\right)$$

$$+\sum_{j=1}^{N}\sum_{r=1}^{n} a_j \frac{\pi\left[1-\left(q_r^b\right)^2\right]}{n+1} g_y^{(j)}\left(q_r^b\right) G_{\sigma_{xy}}^{y}\left(x-x_j\left(q_r^b\right), y-y_j\left(q_r^b\right)\right)$$

$$+\sum_{j=1}^{N}\sum_{r=1}^{n} a_j \frac{\pi}{n} g_{\phi}^{(j)}\left(q_r^u\right) G_{\sigma_{yy}}^{\phi}\left(x-x_j\left(q_r^u\right), y-y_j\left(q_r^u\right)\right)+\sigma_{yy}^{0}(x,y),$$

$$m_{yz}(x,y)=\sum_{j=1}^{N}\sum_{r=1}^{n} a_j \frac{\pi\left[1-\left(q_r^b\right)^2\right]}{n+1} g_x^{(j)}\left(q_r^b\right) G_{m_{yz}}^{x}\left(x-x_j\left(q_r^b\right), y-y_j\left(q_r^b\right)\right)$$

$$+\sum_{j=1}^{N}\sum_{r=1}^{n} a_j \frac{\pi\left[1-\left(q_r^b\right)^2\right]}{n+1} g_y^{(j)}\left(q_r^b\right) G_{m_{yz}}^{y}\left(x-x_j\left(q_r^b\right), y-y_j\left(q_r^b\right)\right)$$

$$+\sum_{j=1}^{N}\sum_{r=1}^{n} a_j \frac{\pi}{n} g_{\phi}^{(j)}\left(q_r^u\right) G_{m_{yz}}^{\phi}\left(x-x_j\left(q_r^u\right), y-y_j\left(q_r^u\right)\right) \tag{36}$$

As shown in Eq (27), the stress component m_{yz} is square root singular at crack tips. The couple stress intensity factors (CSIFs) are defined as

$$K_R^{(i)} = \lim_{p\to 1^+}\left[\sqrt{2(p-1)}\, m_{yz}\left(x_i(p), y_i(p)\right)\right]$$

$$K_L^{(i)} = \lim_{p\to -1^-}\left[\sqrt{-2(p+1)}\, m_{yz}\left(x_i(p), y_i(p)\right)\right] \tag{37}$$

Therefore, from last Eq (30) and Eq (37), CSIFs under in-plane deformation may be obtained as

$$\left\{K_R^{(i)}, K_L^{(i)}\right\} = \frac{Gl^2}{2}\left\{-g_\phi^{(i)}(1), g_\phi^{(i)}(-1)\right\} \tag{38}$$

6. Numerical results

In the sequel, we consider elastic planes under uniform traction as $|y| \to \infty$. Therefore, in the absence of cracks, couple stress tensor vanishes. Numerical results of stress components are provided for three different values of l/a, along a crack line outside the crack surface. Moreover, Eq (38) is used to determine the normalized CSIFs, $(K_L, K_R)/\sigma_0 a^{3/2}$, where σ_0 is a component of applied traction and subscripts L and R signify crack tips, $(-a, 0)$ and $(a, 0)$, respectively.

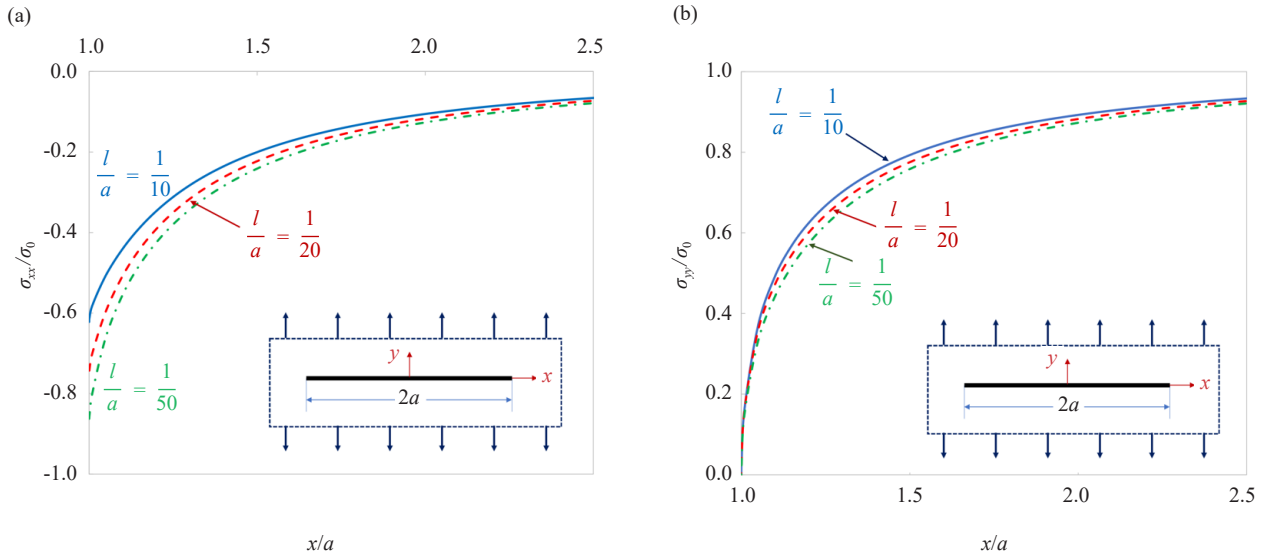

Figure 2. Normalized stress on the x-axis, outside crack under normal traction

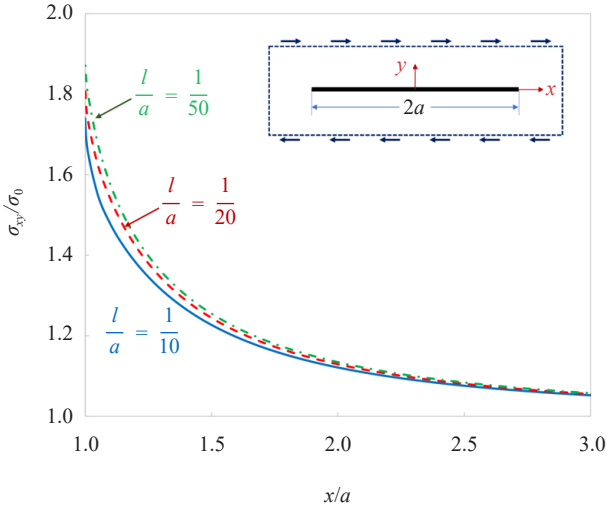

Figure 3. Normalized stress on the x-axis, outside crack under shear traction

In this section, the analysis of a plane weakened by a horizontal crack with length $2a$, sustaining normal traction $t_{yy}(x, y) = \sigma_0$ as $|y| \to \infty$, is taken up. The right side of integral Eq (35) are, $t_{xy}(p_k^b) = m_{yz}(p_l^u) = 0$, $\sigma_{yy}(p_k^b) = -\sigma_0$. In-plane normalized stresses $\sigma_{xx}(x, 0)/\sigma_0$, $\sigma_{yy}(x, 0)/\sigma_0$ for different values of intrinsic length l are shown in Figure 2. As the result of symmetry, $\sigma_{xy}(x, 0) = 0$. At a crack tip, the stress component $\sigma_{xx}(x, 0)$ is bounded and its value attenuates as l increases. From Eq (19), the traction-free boundary conditions on the crack surface $-a \le x \le a$ yield, $t_{yy}(x, 0) = \sigma_{yy}(x, 0) = 0$. Therefore, at a crack tip, only bounded stress component σ_{xx} exists. The normalized CSIFs (Table 1) at the tips of the crack are equal.

Table 1. CSIFs under in-plane traction

Example	CSIF	$l = 1/10$	$l = 1/20$	$l = 1/50$
Crack under normal traction	$(K_R = K_L)/\sigma_0\sqrt{a}$	3.03×10^{-3}	8.29×10^{-4}	1.47×10^{-4}
Collinear cracks	$K_R/\sigma_0\sqrt{a}$	1.41×10^{-3}	3.83×10^{-4}	1.72×10^{-4}
	$K_L/\sigma_0\sqrt{a}$	-2.90×10^{-3}	-8.01×10^{-4}	-5.05×10^{-4}
Non-collinear cracks	$K_R/\sigma_0\sqrt{a}$	1.99×10^{-3}	4.62×10^{-4}	5.54×10^{-5}
	$K_L/\sigma_0\sqrt{a}$	-2.85×10^{-3}	-7.78×10^{-4}	-2.70×10^{-4}

In this example, the plane under uniformly distributed far-field shear traction $t_{xy}(x, y) = \tau_0$ as $|y| \to \infty$, weakened by a crack, is analyzed in Figure 3. The only non-vanishing stress component along the crack line is the shear stress $\sigma_{xy}(x, 0)$, $|x| > a$. Furthermore, due to anti-symmetry CSIF does not exist. The value of l, except for $l = 0$, wherein $\sigma_{xy}(x, 0)$ is unbounded as $x \to a^+$, weakly affects the stress component.

We investigate the interaction between two collinear cracks in a plane under uniform traction components $t_{yy} = \sigma_0$ and $t_{xy} = \sigma_0/2$. The normalized stress components on the x-axis are shown in Figures 4(a-f). The extremum of stress components, on the ligament between cracks tips, occurs at the middle of the ligament. In this region, the intrinsic length l changes only the values not the behavior of the stress field. On the half-line $x < -a$, the effect of l is negligible. Table 1 contains the normalized CSIFs.

In the last example, the interaction between two parallel off-center cracks, under remote normal traction $t_{yy} = \sigma_0$ is studied. The variations of stress components on the x-axis are shown in Figures 5(a-f). Comparing the results on the x-axis for $x < -a$ with those of the first example shows the appearance of a weak shear stress component whereas normal stress components $\sigma_{xx}(x, 0)$ and $\sigma_{yy}(x, 0)$ have changed slightly. On the half-line $x > a$, contrary to stress components $\sigma_{yy}(x, 0)$ and $\sigma_{xy}(x, 0)$, the behavior of $\sigma_{xx}(x, 0)$ changes with the value of l/a. On the half-line, however, the extremum of all stress components enhances significantly as l decreases. The normalized CSIFs are given in Table 1. In the case of two parallel interacting micro-cracks, the signs of CSIFs at the tips of a crack are different.

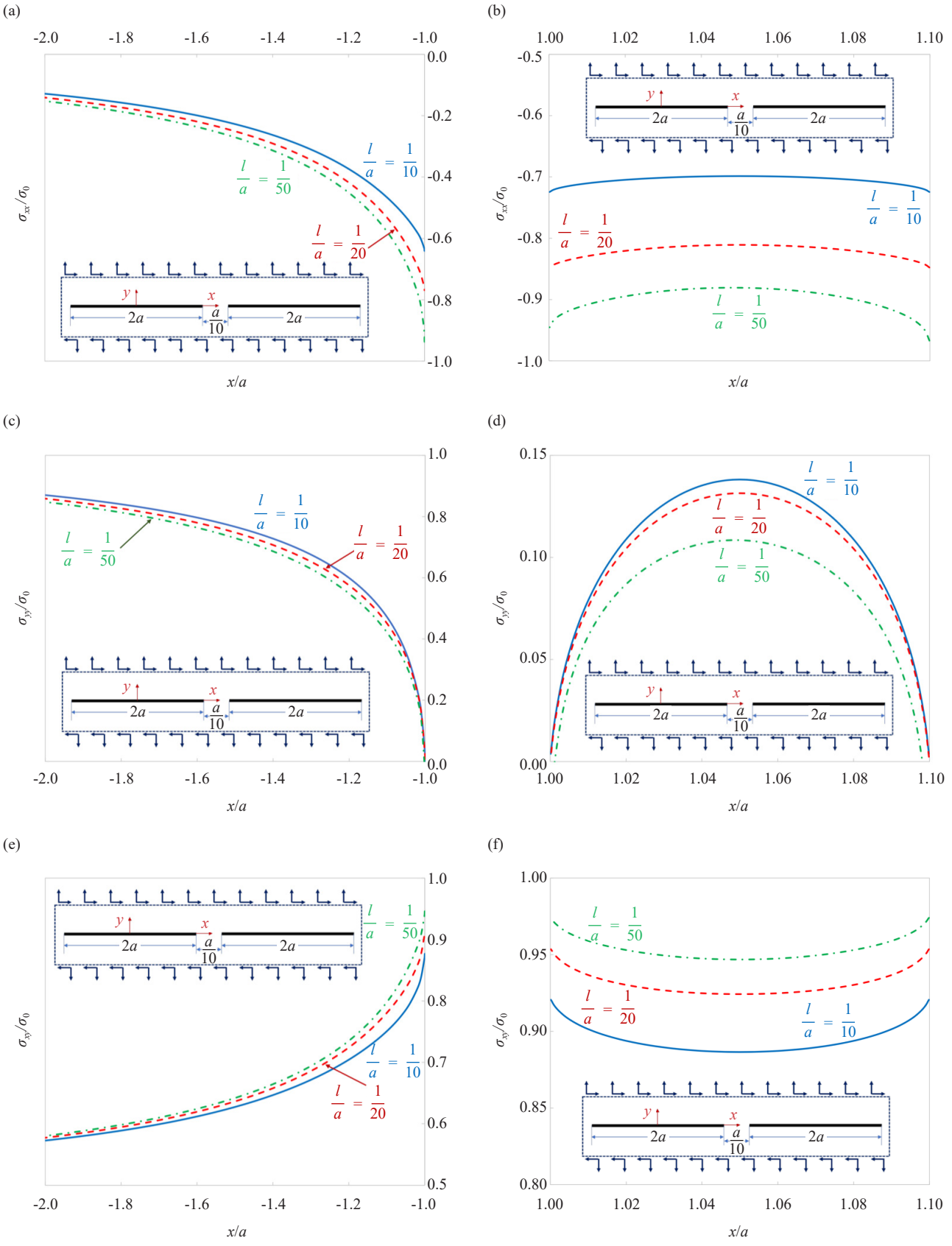

Figure 4. Normalized stress components on the line $y = 0$ for two co-linear cracks under uniform normal and shear tractions, (a, c, e) outside cracked area, (b, d, f) on ligament between cracks

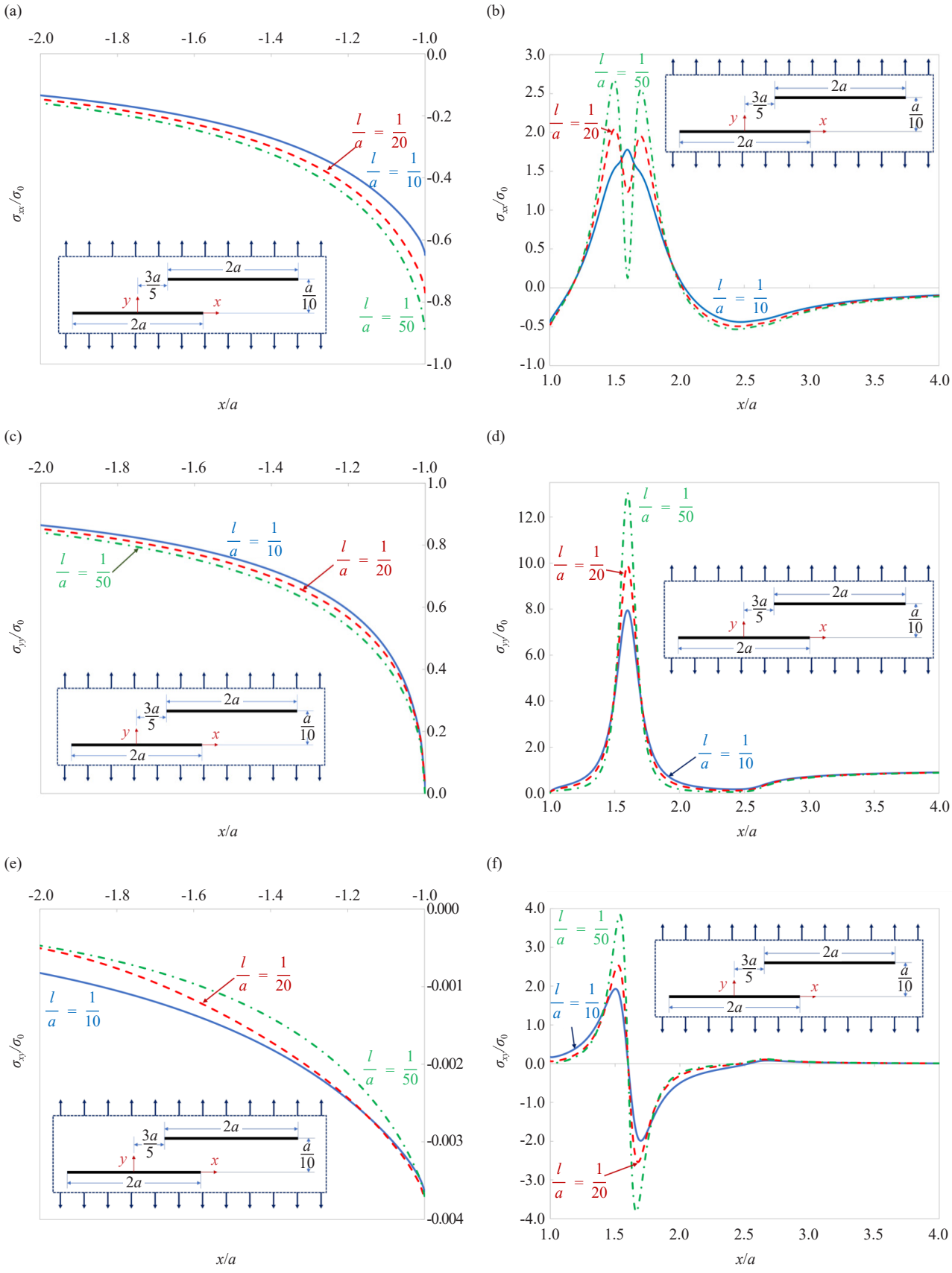

Figure 5. Normalized stress components outside of the crack surface on the *x*-axis for two parallel off-center cracks under uniform normal traction

7. Conclusion

The Volterra edge dislocation and wedge disclination are analyzed in an isotropic elastic plane employing the modified couple-stress theory. The stress field for an edge dislocation is Cauchy singular. Utilizing the Williams procedure reveals that in the modified couple stress theory, the stress field at a crack tip, is bounded but the couple stress tensor is square root singular. The dislocation solution in conjunction with the distributed dislocation technique is utilized to construct singular integral equations to analyze N interacting parallel micro-cracks. The equations are solved numerically for the density of dislocations on a crack surface. Several examples of a single and two interacting cracks are solved and stress distribution along the crack lines together with the normalized CSIFs at the tips of cracks for three values of the material intrinsic length-scale l are determined. In all examples, as the value of length scale l decreases CSIFs attenuate while the stress field near the crack tips experiences significant growth.

Moreover, the length scale, except for $\sigma_{xx}(x, 0)$, $x > a$ in the case of two parallel off-center cracks, has little effect on the behavior of the stress field. It is worth mentioning that in the case of two interacting cracks, signs of the CSIFs at the tips of a crack differ. Furthermore, $|K_L| > |K_R|$; therefore, CSIF is more severe at the crack tip which is farther from the tips of other interacting cracks.

Conflict of interest

The authors have no competing interests to declare that are relevant to the content of this article.

References

[1] S. Nikolov, C.-S. Han, and D. Raabe, "On the origin of size effects in small-strain elasticity of solid polymers," *International Journal of Solids and Structures*, vol. 44, no. 5, pp. 1582-1592, 2007.

[2] R. S. Lakes, "Size effects and micromechanics of a porous solid," *Journal of Materials Science*, vol. 18, pp. 2572-2580, 1983.

[3] R. Lakes and K. Elms, "Indentability of conventional and negative Poisson's ratio foams," *Journal of Composite Materials*, vol. 27, no. 12, pp. 1193-1202, 1993.

[4] A. C. Eringen, C. Speziale, and B. Kim, "Crack-tip problem in non-local elasticity," *Journal of the Mechanics and Physics of Solids*, vol. 25, no. 5, pp. 339-355, 1977.

[5] M. A. Roudbari, T. D. Jorshari, C. Lü, R. Ansari, A. Z. Kouzani, and M. Amabili, "A review of size-dependent continuum mechanics models for micro-and nano-structures," *Thin Walled Structures*, vol. 170, pp. 108562, 2022.

[6] E. Sternberg and R. Muki, "The effect of couple-stresses on the stress concentration around a crack," *International Journal of Solids and Structures*, vol. 3, no. 1, pp. 69-95, 1967.

[7] R. Mindlin, "Influence of couple-stresses on stress concentrations," *Experimental Mechanics*, vol. 3, no. 1, pp. 1-7, 1963.

[8] S. Han, M. Narasimhan, and T. Kennedy, "Dynamic propagation of a finite crack in a micropolar elastic solid," *Acta Mechanica*, vol. 85, no. 3, pp. 179-191, 1990.

[9] I. Vardoulakis, G. Exadaktylos, and E. Aifantis, "Gradient elasticity with surface energy: mode-III crack problem," *International Journal of Solids and Structures*, vol. 33, no. 30, pp. 4531-4559, 1996.

[10] Y. Huang, L. Zhang, T. Guo, and K.-C. Hwang, "Mixed mode near-tip fields for cracks in materials with strain-gradient effects," *Journal of the Mechanics and Physics of Solids*, vol. 45, no. 3, pp. 439-465, 1997.

[11] J. Chen, Y. Huang, and M. Ortiz, "Fracture analysis of cellular materials: a strain gradient model," *Journal of the Mechanics and Physics of Solids*, vol. 46, no. 5, pp. 789-828, 1998.

[12] G. Paulino, A. Fannjiang, and Y. S. Chan, "Gradient elasticity theory for mode III fracture in functionally graded materials-part I: crack perpendicular to the material gradation," *Journal of Applied Mechanics*, vol. 70, no. 4, pp. 531-542, 2003.

[13] Y.-S. Chan, G. H. Paulino, and A. C. Fannjiang, "Gradient elasticity theory for mode III fracture in functionally graded materials-part II: crack parallel to the material gradation," *Journal of Applied Mechanics*, vol. 75, no. 6, pp. 061015, 2008.

[14] W. Koiter, "Couple-stresses in the theory of elasticity, I & II," *Proceedings of the Koninklijke Nederlandse*

Akademie Van Wetenschappen, vol. 67, pp. 17-44, 1964.
[15] A. Piccolroaz, G. Mishuris, and E. Radi, "Mode III interfacial crack in the presence of couple-stress elastic materials," *Engineering Fracture Mechanics*, vol. 80, pp. 60-71, 2012.
[16] G. Mishuris, A. Piccolroaz, and E. Radi, "Steady-state propagation of a mode III crack in couple stress elastic materials," *International Journal of Engineering Science*, vol. 61, pp. 112-128, 2012.
[17] S. Itou, "Effect of couple-stresses on the stress intensity factor for a crack in an infinite elastic strip under tension," *European Journal of Mechanics A/Solids*, vol. 42, pp. 335-343, 2013.
[18] I. Karimipour and A. R. Fotuhi, "Anti-plane analysis of an infinite plane with multiple cracks based on strain gradient theory," *Acta Mechanica*, vol. 228, pp. 1793-1817, 2017.
[19] B. Zhao, T. Liu, J. Pan, X. Peng, and X. Tang, "A stress analytical solution for mode III crack within modified gradient elasticity," *Mechanics Research Communications*, vol. 84, pp. 142-147, 2017.
[20] K. Baxevanakis, P. Gourgiotis, and H. Georgiadis, "Interaction of cracks with dislocations in couple-stress elasticity. Part I: Opening mode," *International Journal of Solids and Structures*, vol. 118, pp. 179-191, 2017.
[21] K. Baxevanakis, P. Gourgiotis, and H. Georgiadis, "Interaction of cracks with dislocations in couple-stress elasticity. part II: Shear modes," *International Journal of Solids and Structures*, vol. 118, pp. 192-203, 2017.
[22] J. P. Vafa and S. J. Fariborz, "Analysis of micro-cracks using modified couple-stress elasticity under anti-plane deformation," *Solid State Phenomena*, vol. 258, pp. 182-185, 2017.
[23] P. A. Gourgiotis, "Interaction of shear cracks in microstructured materials modeled by couple-stress elasticity," *Journal of Mechanics of Materials and Structures*, vol. 13, no. 3, pp. 401-419, 2018.
[24] M. Homayounfard, A. Daneshmehr, and A. Salari, "A finite element formulation for crack problem in couple-stress elasticity," *International Journal of Applied Mechanics*, vol. 10, no. 2, pp. 1850018, 2018.
[25] R. P. Joseph, B. Wang, and B. Samali, "Size effects on double cantilever beam fracture mechanics specimen based on strain gradient theory," *Engineering Fracture Mechanics*, vol. 169, pp. 309-320, 2017.
[26] J. Li and B. Wang, "Fracture mechanics analysis of an anti-plane crack in gradient elastic sandwich composite structures," *International Journal of Mechanics and Materials in Design*, vol. 15, pp. 507-519, 2019.
[27] A. Gharahi and P. Schiavone, "Edge dislocation with surface flexural resistance in micropolar materials," *Acta Mechanica*, vol. 230, no. 5, pp. 1513-1527, 2019.
[28] A. Nobili, E. Radi, and A. Vellender, "Diffraction of antiplane shear waves and stress concentration in a cracked couple stress elastic material with micro inertia," *Journal of the Mechanics and Physics of Solids*, vol. 124, pp. 663-680, 2019.
[29] K. P. Baxevanakis and H. Georgiadis, "A displacement-based formulation for interaction problems between cracks and dislocation dipoles in couple-stress elasticity," *International Journal of Solids and Structures*, vol. 159, pp. 1-20, 2019.
[30] A. E. Giannakopoulos and T. Zisis, "Uniformly moving antiplane crack in flexoelectric materials," *European Journal of Mechanics A/Solids*, vol. 85, pp. 104136, 2021.
[31] X. Tian, M. Xu, H. Zhou, Q. Deng, Q. Li, J. Sladek, and V. Sladek, "Analytical studies on mode III fracture in flexoelectric solids," *Journal of Applied Mechanics*, vol. 89, no. 4, pp. 041006, 2022.
[32] J. Lei, X. Wei, P. Ding, and C. Zhang, "General displacement and traction BEM for plane couple-stress problems," *Engineering Analysis with Boundary Elements*, vol. 140, pp. 59-69, 2022.
[33] P. H. Cong and D. H. Duc, "Phase field model for fracture based on modified couple stress," *Engineering Fracture Mechanics*, vol. 269, pp. 108534, 2022.
[34] J. Chen, Y.-W. Wang, and X.-F. Li, "A mode-I crack embedded in a prestressed material with microstructure," *European Journal of Mechanics A/Solids*, vol. 100, pp. 104990, 2023.
[35] J. Chen, Y. Wang, R. Zheng, and X. Li, "Mode-III interface crack in a bi-material with initial stress and couple stress," *Engineering Fracture Mechanics*, vol. 281, pp. 109135, 2023.
[36] M. Lazar, "Dislocations in nonlocal simplified strain gradient elasticity: Eringen meets aifantis," *International Journal of Mechanical Sciences*, vol. 275, pp. 109294, 2024.
[37] Y. Solyaev, "Higher-order asymptotic crack-tip fields in simplified strain gradient elasticity," *Theoretical and Applied Fracture Mechanics*, vol. 130, pp. 104321, 2024.
[38] J. Chen, Y.-W. Wang, and X.-F. Li, "Moving mode-III crack under bending and twisting couple stress," *Engineering Fracture Mechanics*, vol. 308, pp. 110335, 2024.
[39] J. Xie and C. Linder, "Full field crack solutions in anti-plane flexoelectricity," *Theoretical and Applied Fracture Mechanics*, vol. 134, pp. 104674, 2024.
[40] C. Knisovitis, A. E. Giannakopoulos, and A. J. Rosakis, "Anti-plane yoffe-type crack in flexoelectric material,"

Engineering Fracture Mechanics, vol. 311, pp. 110551, 2024.
[41] F. Yang, A. Chong, D. C. C. Lam, and P. Tong, "Couple stress based strain gradient theory for elasticity," *International Journal of Solids and Structures*, vol. 39, no. 10, pp. 2731-2743, 2002.
[42] D. A. Hills, P. A. Kelly, D. N. Dai, and A. M. Korsunsky, *Solution of Crack Problems: The Distributed Dislocation Technique*. Dordrecht, the Netherlands: Springer, 2013.
[43] N. Fleck, G. Muller, M. F. Ashby, and J. W. Hutchinson, "Strain gradient plasticity: theory and experiment," *Acta Metallurgica et Materialia*, vol. 42, no. 2, pp. 475-487, 1994.
[44] Z. Li, Y. He, J. Lei, S. Guo, D. Liu, and L. Wang, "A standard experimental method for determining the material length scale based on modified couple stress theory," *International Journal of Mechanical Sciences*, vol. 141, pp. 198-205, 2018.
[45] Z. Y. Wu and S. P. Li, "The generalized plane strain problem and its application in three-dimensional stress measurement," *International Journal of Rock Mechanics and Mining Sciences & Geomechanics Abstracts*, vol. 27, no. 1, pp. 43-49, 1990.
[46] M. L. Williams, "On the stress distribution at the base of a stationary crack," *Journal of Applied Mechanics*, vol. 24, pp. 109-114, 1957.
[47] N. Aravas and A. Giannakopoulos, "Plane asymptotic crack-tip solutions in gradient elasticity," *International Journal of Solids and Structures*, vol. 46, no. 2526, pp. 4478-4503, 2009.
[48] M. Abramowitz and I. A. Stegun, *Handbook of Mathematical Functions with Formulas, Graphs, and Mathematical Tables (Applied Mathematics Series 55)*. Washington, DC: National Bureau of Standards, 1972.
[49] F. Erdogan, G. D. Gupta, and T. S. Cook, "Numerical solution of singular integral equations" in *Methods of Analysis and Solutions of Crack Problems (Mechanics of Fracture, Vol. 1)*, G. C. Sih, Ed. Dordrecht, the Netherlands: Springer, 1973, pp. 368-425.

Appendix A

The following identities are used for the determination of displacement components

$$\int_0^\infty e^{-\beta|y|}\cos(\beta x)d\beta=\frac{|y|}{r^2},\ \int_0^\infty e^{-\beta|y|}\sin(\beta x)d\beta=\frac{x}{r^2}$$

$$\int_0^\infty \beta e^{-\beta|y|}\cos(\beta x)d\beta=\frac{y^2-x^2}{r^4},\ \int_0^\infty \beta e^{-\beta|y|}\sin(\beta x)d\beta=\frac{2x|y|}{r^4}$$

$$\int_0^\infty \frac{1}{\beta}e^{-\beta|y|}\sin(\beta x)d\beta=\tan^{-1}\left(\frac{x}{|y|}\right)$$

$$\int_0^\infty e^{-|y|\sqrt{\frac{4}{l^2}+\beta^2}}\cos(\beta x)d\beta=\frac{2}{l}\frac{|y|}{r}K_1\left(\frac{2}{l}r\right),\ \int_0^\infty \beta e^{-|y|\sqrt{\frac{4}{l^2}+\beta^2}}\sin(\beta x)d\beta=\frac{4x|y|}{l^2r^2}K_2\left(\frac{2}{l}r\right)$$

$$\int_0^\infty \sqrt{\frac{4}{l^2}+\beta^2}\,e^{-|y|\sqrt{\frac{4}{l^2}+\beta^2}}\cos(\beta x)d\beta=\frac{4}{l^2}\frac{y^2}{r^2}K_0\left(\frac{2}{l}r\right)+\left(\frac{4}{l}\frac{y^2}{r^3}-\frac{2}{l}\frac{1}{r}\right)K_1\left(\frac{2}{l}r\right)$$

$$\int_0^\infty \frac{\beta^2}{\sqrt{\frac{4}{l^2}+\beta^2}}e^{-|y|\sqrt{\frac{4}{l^2}+\beta^2}}\cos(\beta x)d\beta=-\left[\frac{4}{l^2}\frac{x}{r^2}^2K_0\left(\frac{2}{l}r\right)+\frac{2}{l}\frac{x^2-y^2}{r^3}K_1\left(\frac{2}{l}r\right)\right]$$

Appendix B

The kernels of the integral equations (30) and (36) are

$$\bar{G}^{x}_{t_{xy}}(x)=-\frac{G}{\pi}\left\{\left(\frac{2\omega+3}{\omega+2}\right)\frac{1}{x}+\left[\frac{2}{x}K_0\left(\frac{2}{l}|x|\right)+\frac{2}{l}\frac{|x|}{x^3}\left(l^2+2x^2\right)K_1\left(\frac{2}{l}|x|\right)-\frac{1}{x}-\frac{l^2}{x^3}\right]\right\}$$

$$\bar{G}^{y}_{\sigma_{yy}}(x)=-\frac{G}{\pi}\left\{\left(\frac{2\omega+3}{\omega+2}\right)\frac{1}{x}-\frac{2}{x}K_2\left(\frac{2}{l}|x|\right)-\frac{1}{x}+\frac{l^2}{x^3}\right\}$$

$$\bar{G}^{\phi}_{\sigma_{yy}}(x)=\frac{Gl}{\pi}\left\{\frac{|x|}{x^2}K_1\left(\frac{2}{l}|x|\right)-\frac{l}{2x^2}\right\}$$

$$\bar{G}^{y}_{m_{yz}}(x)=-\frac{Gl}{2\pi}\left\{\frac{|x|}{x^2}K_1\left(\frac{2}{l}|x|\right)-\frac{l}{2x^2}\right\}$$

$$\bar{G}^{\phi}_{m_{yz}}(x)=-\frac{Gl}{2\pi}\left[\frac{l}{x}+\pi+l\int_0^{\infty}\frac{1}{\beta l}\left(\sqrt{\beta^2l^2+4}-\beta l\right)\sin(\beta x)d\beta\right]$$

$$G^{x}_{\sigma_{xx}}(x,y)=\frac{G}{\pi}y\left\{\frac{3x^2-y^2}{r^4}\left[2K_0\left(\frac{2r}{l}\right)-\frac{l^2}{r^2}\right]+\frac{2}{l}\left[\frac{2x^2}{r^3}+\frac{l^2\left(3x^2-y^2\right)}{r^5}\right]K_1\left(\frac{2r}{l}\right)+\left(\frac{\omega+1}{\omega+2}\right)\frac{3x^2+y^2}{r^4}\right\}$$

$$G^{y}_{\sigma_{xx}}(x,y)=-\frac{G}{\pi}x\left\{\frac{x^2-3y^2}{r^4}\left[2K_0\left(\frac{2r}{l}\right)-\frac{l^2}{r^2}\right]-\frac{2}{l}\left[\frac{2y^2}{r^3}-\frac{l^2\left(x^2-3y^2\right)}{r^5}\right]K_1\left(\frac{2r}{l}\right)+\left(\frac{\omega+1}{\omega+2}\right)\frac{x^2-y^2}{r^4}\right\}$$

$$G^{\phi}_{\sigma_{xx}}(x,y)=\frac{G}{\pi}\left\{\frac{2y^2}{r^2}K_0\left(\frac{2r}{l}\right)+\frac{l^2}{2}\frac{x^2-y^2}{r^4}\left[1-\frac{2r}{l}K_1\left(\frac{2r}{l}\right)\right]\right\}$$

$$G^{x}_{\sigma_{yy}}(x,y)=-\frac{G}{\pi}y\left\{\frac{3x^2-y^2}{r^4}\left[2K_0\left(\frac{2r}{l}\right)-\frac{l^2}{r^2}\right]+\frac{2}{l}\left[\frac{2x^2}{r^3}+\frac{l^2\left(3x^2-y^2\right)}{r^5}\right]K_1\left(\frac{2r}{l}\right)+\left(\frac{\omega+1}{\omega+2}\right)\frac{x^2-y^2}{r^4}\right\}$$

$$G^{y}_{\sigma_{yy}}(x,y)=\frac{G}{\pi}x\left\{\frac{x^2-3y^2}{r^4}\left[2K_0\left(\frac{2r}{l}\right)-\frac{l^2}{r^2}\right]-\frac{2}{l}\left[\frac{2y^2}{r^3}-\frac{l^2\left(x^2-3y^2\right)}{r^5}\right]K_1\left(\frac{2r}{l}\right)-\left(\frac{\omega+1}{\omega+2}\right)\frac{x^2+3y^2}{r^4}\right\}$$

$$G^{\phi}_{\sigma_{yy}}(x,y)=-\frac{G}{\pi}\left\{\frac{2y^2}{r^2}K_0\left(\frac{2r}{l}\right)+\frac{l^2\left(x^2-y^2\right)}{2r^4}\left[1-\frac{2r}{l}K_1\left(\frac{2r}{l}\right)\right]\right\}$$

$$G^{x}_{\sigma_{xy}}(x,y)=-\frac{G}{\pi}x\left\{\frac{x^2-3y^2}{r^4}\left[2K_0\left(\frac{2r}{l}\right)-\frac{l^2}{r^2}\right]+\frac{2}{l}\left[\frac{x^2-y^2}{r^3}+\frac{l^2\left(x^2-3y^2\right)}{r^5}\right]K_1\left(\frac{2r}{l}\right)+\left(\frac{\omega+1}{\omega+2}\right)\frac{x^2-y^2}{r^4}\right\}$$

$$G^{y}_{\sigma_{xy}}(x,y)=-\frac{G}{\pi}y\left\{\frac{3x^2-y^2}{r^4}\left[2K_0\left(\frac{2r}{l}\right)-\frac{l^2}{r^2}\right]+\frac{2}{l}\left[\frac{x^2-y^2}{r^3}+\frac{l^2\left(3x^2-y^2\right)}{r^5}\right]K_1\left(\frac{2r}{l}\right)+\left(\frac{\omega+1}{\omega+2}\right)\frac{x^2-y^2}{r^4}\right\}$$

$$G^{\phi}_{\sigma_{xy}}(x,y)=-G\,\mathrm{sgn}(y)\left[\frac{1}{2}e^{-\frac{2}{l}|y|}-\frac{1}{2\pi}\int_0^{\infty}\left(\beta l^2e^{-\beta|y|}-\frac{\beta^2l^2+2}{\beta}e^{-|y|\sqrt{\frac{4}{l^2}+\beta^2}}\right)\sin(\beta x)d\beta\right]$$

$$G^{x}_{t_{xy}}(x,y)=-\frac{G}{\pi}x\left\{\frac{x^2-3y^2}{r^4}\left[2K_0\left(\frac{2r}{l}\right)-\frac{l^2}{r^2}\right]+\frac{2}{l}\left[\frac{2x^2}{r^3}+\frac{l^2\left(x^2-3y^2\right)}{r^5}\right]K_1\left(\frac{2r}{l}\right)+\left(\frac{\omega+1}{\omega+2}\right)\frac{x^2-y^2}{r^4}\right\}$$

$$G^{y}_{t_{xy}}(x,y)=-\frac{G}{\pi}y\left\{\frac{3x^2-y^2}{r^4}\left[2K_0\left(\frac{2r}{l}\right)-\frac{l^2}{r^2}\right]+\frac{2}{l}\left[\frac{2x^2}{r^3}+\frac{l^2\left(3x^2-y^2\right)}{r^5}\right]K_1\left(\frac{2r}{l}\right)+\left(\frac{\omega+1}{\omega+2}\right)\frac{x^2-y^2}{r^4}\right\}$$

$$G^{\phi}_{t_{xy}}(x,y)=\frac{G}{\pi}\frac{xy}{r^2}\left[\frac{l^2}{r^2}-2K_2\left(\frac{2r}{l}\right)\right]$$

$$G^{x}_{m_{yz}}(x,y)=\frac{G}{\pi}\frac{xy}{r^2}\left[K_2\left(\frac{2r}{l}\right)-\frac{l^2}{2r^2}\right]$$

$$G^{y}_{m_{yz}}(x,y)=\frac{G}{\pi}\left\{\frac{y^2}{r^2}K_0\left(\frac{2r}{l}\right)+\frac{l^2\left(x^2-y^2\right)}{4r^4}\left[1-\frac{2r}{l}K_1\left(\frac{2r}{l}\right)\right]\right\}$$

$$G^{\phi}_{m_{yz}}(x,y)=-\frac{Gl}{2\pi}\left[\frac{lx}{r^2}+\pi e^{-\frac{2}{l}|y|}+l\int_0^{\infty}\left(\frac{1}{\beta}\sqrt{\frac{4}{l^2}+\beta^2}\,e^{-|y|\sqrt{\frac{4}{l^2}+\beta^2}}-e^{-\beta|y|}\right)\sin(\beta x)d\beta\right]$$